

# Quantitative measurement of aging using image texture entropy

Lior Shamir \*, Catherine A. Wolkow and Ilya G. Goldberg

Laboratory of Genetics, National Institute on Aging/NIH

Received on XXXXX; revised on XXXXX; accepted on XXXXX

Associate Editor: XXXXXXXX

## ABSTRACT

**Motivation:** A key element in understanding the aging of *C. elegans* is objective quantification of the morphological differences between younger and older animals. Here we propose to use the image texture entropy as an objective measurement that reflects the structural deterioration of the *C. elegans* muscle tissues during aging.

**Results:** The texture entropy and directionality of the muscle microscopy images were measured using 50 animals on day 0, 2, 4, 6, 8, 10, and 12 of adulthood. Results show that the entropy of the *C. elegans* pharynx tissues increases as the animal ages, but a sharper increase was measured between day two and day four, and between day eight and day 10. These results are in agreement with gene expression findings, and support the contention that the process of *C. elegans* aging has several distinct stages. This can indicate that *C. elegans* aging is driven by developmental pathways, rather than stochastic accumulation of damage.

**Availability:** The image data are freely available on the internet at <http://ome.grc.nia.nih.gov/iicbu2008/celegans>, and the Haralick and Tamura texture analysis source code can be downloaded at <http://ome.grc.nia.nih.gov/wnd-charm>.

**Contact:** shamirl@mail.nih.gov

## 1 INTRODUCTION

While aging is one of the most prevalent biological processes in nature, little is yet known about the mechanisms that affect or cause aging. To effectively study the process of aging, it is required to be able to objectively quantify the age of the studied organism. While the chronological age of an organism is trivial to measure, it provides a weak link to the actual physiological age. Therefore, a quantitative method that can objectively measure the physiological age is required.

*Caenorhabditis elegans* is a powerful model for the study of aging (Golden & Melov, 2006). One of the primary advantages of *C. elegans* as an experimental organism is that during its life-span of two to three weeks, the functional and morphological aging of the muscle tissues can be easily observed through a microscope. These changes can be noticed when observing the pharynx terminal bulb of the *C. elegans*. Figure 1 shows typical images of the terminal bulb in day 0, 2, 4, 6, 8, 10 and 12 of adulthood, taken using differential interference contrast (DIC) microscopy with a 40x objective.

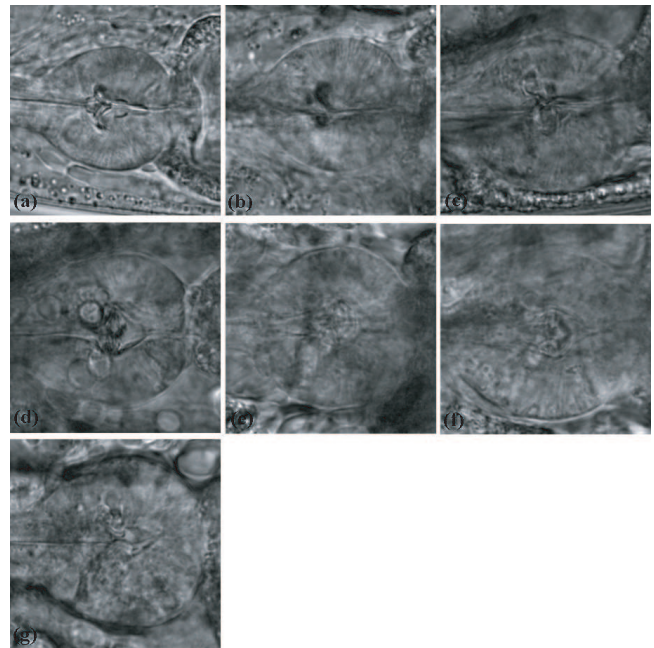


**Fig. 1.** Microscopy images of the terminal bulb of *C. elegans* in (a) day 0, (b) day 2, (c) day 4, (d) day 6, (e) day 8, (f) day 10, (g) day 12 of adulthood

Clearly, the process of aging is accompanied by a noticeable and obvious functional decline, which is particularly reflected by the loss of muscle mass. As Figure 1 shows, in day two and zero the terminal bulb is noticeably more structured than in days 10 and 12, where the muscle tissues deteriorate and the entropy increases. The process of muscle mass loss is referred to as *sarcopenia*. The cause for the structural and functional decline of the *C. elegans* pharynx and terminal bulb is yet unknown (Wolkow, 2006).

Some attempts have been made to manually score muscle tissue morphology in order to quantify aging (Herndon *et al.*, 2002; Gari-gan *et al.*, 2002; Helfrich *et al.*, 2007). However, manual scoring of muscle tissues is subjected to the bias introduced by the human decision-making, and is limited by what the human eye can perceive. Moreover, even in cases where the unaided human eye can tell between a young and an older muscle tissue, it becomes highly difficult for a person to measure the differences in a quantitative fashion.

\*to whom correspondence should be addressed

A more recent attempt to quantify aging applied an image classifier that utilized several hundreds distinct image features working in concert, and weighted by their statistical discrimination power such that the chronological age was used as the gold standard (Johnston *et al.*, 2008). That experiment showed that the *C. elegans* pharynx proceeds through several distinct stages during aging.

A different approach to study the process of aging used DNA microarrays to monitor the expression of age-regulated genes (Budovskaya *et al.*, 2008), indicating that the process of aging is driven by developmental pathways rather than accumulation of damage.

Here we propose to quantify the process of the muscle tissue structural deterioration by measuring the texture entropy using microscope images of the *C. elegans* pharynx. This method can be used to show that distinct states that have been observed by DNA microarray experiments are in agreement with the muscle tissue deterioration reflected by the texture entropy of *C. elegans* microscopy images. This finding supports the contention that the aging of *C. elegans* has several distinct states, which are separated by periods of rapid aging.

## 2 METHODS

The entropy of the images was quantified by using the Haralick texture features (Haralick *et al.*, 1973). The key element of the Haralick features is the gray-level co-occurrence matrix. In the co-occurrence matrix, the entry  $i, j$  of the co-occurrence matrix  $M_d$  is the number of occurrences of gray levels  $i$  and  $j$  such that the distance between them is  $d$  pixels. The co-occurrence matrix is described by Equation 1.

$$M_d(i, j) = |[(r, s), (t, v)] : I(r, s) = i, I(t, v) = j|, \quad (1)$$

where  $(r, s), (t, v) \in \mathbb{N} \times \mathbb{N}$  and  $(t, v) = (r + dx, s + dy)$ .

The co-occurrence matrix can be used to compute useful texture features (Haralick *et al.*, 1973). In this study we use the Haralick texture entropy, which quantitatively measures the randomness of the gray-level distribution, and defined by  $\sum_i \sum_j M_d(i, j) \log M_d(i, j)$ . In the images taken at different time point shown in Figure 1 it can be noticed that the terminal bulb generally becomes less structured and more chaotic as the worm gets older. Therefore, the quantitative measurement of the Haralick texture entropy can reflect the decline of the muscle tissues of the terminal bulb that can be visually observed by using a microscope. In all experiments  $d$  was set to 1, and the dynamic range was reduced into 255 gray levels. The implementation of the Haralick texture analysis used for the experiment was taken from the work of Murphy *et al.* (2001), and is available also as part of the *wndchrm* image analysis tool (Shamir *et al.*, 2008a).

Another measurement that was used in this study is the directionality element of the Tamura texture (Tamura *et al.*, 1978). The Tamura features reflect textures in a numerical fashion that is based on the human perception, and consist of three primary descriptors, which are the *contrast*, *coarseness*, and *directionality*. *Coarseness* refers to texture granularity, reflected by the size and number of texture primitives. A coarse texture contains a small number of large primitives, while a fine texture contains a large number of small primitives. *Contrast* refers to the difference in intensity among neighboring pixels. A texture of high contrast has large difference in intensity among neighboring pixels, while a texture of low contrast has small difference. A detailed description of the tamura texture can be found in (Tamura *et al.*, 1978; Lin *et al.*, 2003).

In this study we use the *directionality* element of the Tamura texture, which is a global property of a region that reflects the placement of the

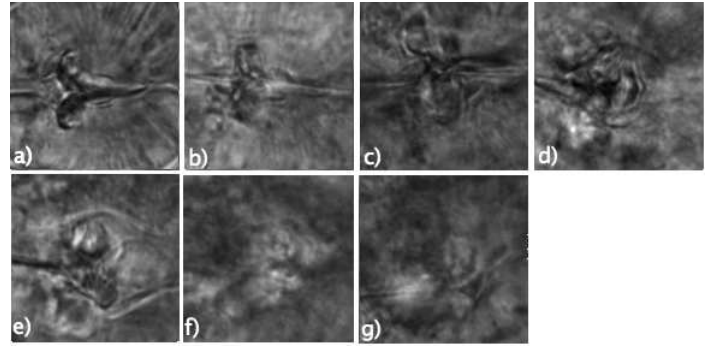


**Fig. 2.** Microscope images of the center of the *C. elegans* terminal bulb in day 0 (a. entropy=1291 directionality=7.36), day 2 (b. entropy=1297 directionality=7.34), day 4 (c. entropy=1338 directionality=7.07), day 6 (d. entropy=1340 directionality=7.07), day 8 (e. entropy=1346 directionality=7.04), day 10 (f. entropy=1420 directionality=6.75), and day 12 (g. entropy=1431 directionality=6.68)

texture primitives. A directional texture, in that sense, has one or more recognizable orientations of primitives, while an isotropic texture has no recognizable orientation of its primitives. The directionality can be computed by Equation 2,

$$f_{dir} = \sum_p^{n_p} \sum_{\phi \in w_p} (\phi - \phi_p)^2 \cdot H_D(\phi), \quad (2)$$

where  $H_D$  is the local direction histogram computed using the Sobel edge operator (Duda & Hart, 1973),  $n_p$  is the number of peaks of  $H_D$ ,  $\phi_p$  is the  $p$ th peak position of  $H_D$ , and  $w_p$  is the range of the  $p$ th peak between valleys. In this study the number of bins for the local direction histogram is 125.

Texture measurement of digital images is a well-studied field, and numerous methods, such as the commonly used Gabor textures (Gabor, 1946), have been proposed. While it can be reasonably assumed that other texture analysis methods can also be informative for this task, we chose to use the Haralick entropy and Tamura directionality, which are intuitive descriptors of the texture structuredness in digital images.

As can be noticed in Figure 1, the straight lines that can be visually seen crossing the terminal bulb become less noticeable as the worm ages, and can barely be seen at all on day 12. Therefore, the directionality of the texture is expected to change gradually as the *C. elegans* gets older, reflecting the decline of the muscle tissues in each time point.

The image dataset used for the experiment was acquired by using differential interference contrast (DIC) microscopy and a 40x objective. The dataset included images of the pharynx region of the worms collected at different ages of day 0, 2, 4, 6, 8, 10, and 12 of adulthood. For each worm, the stage of the microscope was rotated to maintain the same relative orientation in all images. To facilitate production of age-synchronized populations, the worms used in this study carried the *fem-1(hc17)* mutation blocking spermatogenesis. A detailed description about the images can be found in (Johnston *et al.*, 2008), and the dataset can be downloaded freely as part of the IICBU-2008 benchmark suite (Shamir *et al.*, 2008b).

Haralick texture entropy and Tamura texture directionality were computed from a set of  $140 \times 140$  16-bit TIFF images of the center of the *C. elegans* terminal bulb, such that 50 different images (each image from a different animal) were used in each time point. The center of each terminal bulb in the image was determined manually, and provided a uniform set of terminal bulb center images. Figure 2 shows typical images used in this study, and their computed Haralick entropy and Tamura directionality values.

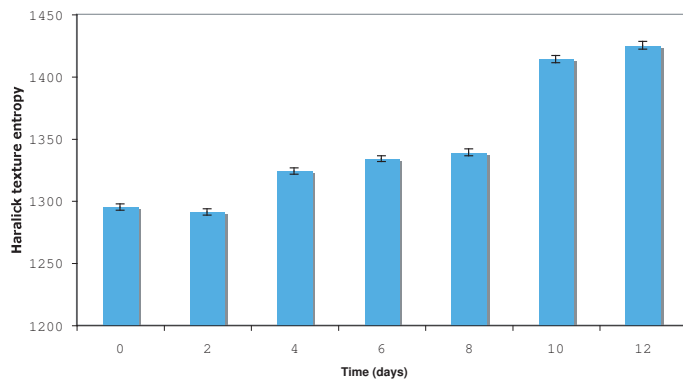


**Fig. 3.** Haralick texture entropy (50 animals) measured using the terminal bulb in day 0, 2, 4, 6, 8, 10, and 12 of adulthood. One leap is noticeable between day two and day four, and another leap between day eight and day 10. The plateau between the two leaps indicate that the muscle decline is slower during that time

### 3 RESULTS

Figure 3 shows the mean and standard error of the Haralick texture entropy computed from the terminal bulb images taken on different days of adulthood. The graph is based on measurements from 50 animals in each time point. As the graph shows, the Haralick texture entropy increases with age, indicating that the terminal bulb becomes less structured and more chaotic as the animal ages. The Pearson correlation between the measured texture entropy and the chronological age is  $\sim 0.69$  ( $P < 0.001$ ).

As can be learned from the graph, while the time difference between each pair of neighboring time-points is constant, it is clear that the measured entropy does not increase linearly to the worm age. Clearly, a leap can be noticed between day two and day four, and a larger leap between day eight and day 10. Days four to six, and 10 to 12 show just minor entropy differences, indicating that the *C. elegans* muscle decline is slower during these periods.

Figure 4 shows the mean of the Tamura texture directionality across the different ages. As before, the values were computed using images of 50 animals for each chronological age. Clearly, the Tamura texture directionality decreases as the worm gets older, showing that the texture of the terminal bulb becomes more sparse in time. The Pearson correlation between the measured Tamura directionality and the chronological age is  $\sim -0.67$  ( $P < 0.001$ ). The Tamura texture directionality increases consistently, but shows two noticeable leaps: one between day two and day four, and another between day eight and day 10.

### 4 DISCUSSION

Here we used the Haralick texture entropy and the Tamura texture directionality to analyze the structural deterioration of the muscle tissues, that can be noticed using DIC microscope images of the *C. elegans* pharynx. These measurements show that the entropy of the image texture increases as the animal gets older, but the rate of the increase is not constant throughout the life of the animal. The experiments revealed two major leaps in the structural deterioration

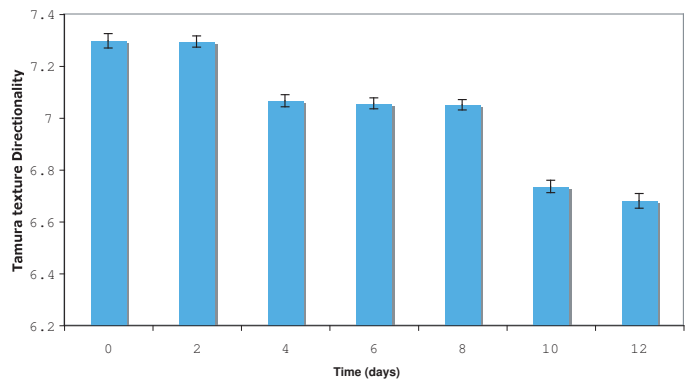


**Fig. 4.** Tamura texture directionality (50 animals) measured using the terminal bulb in day 0, 2, 4, 6, 8, 10, and 12 of adulthood.

of the muscles, one between day two and day four, and the other between day eight and day 10 of adulthood.

Recent experiments using DNA microarrays suggest that the expression of *elt-5*, which is responsible for the expression of a large number of age regulated genes, changes during aging in a non-linear fashion (Budovskaya *et al.*, 2008). The change in the expression of *elt-5::Cherry* reporter in the head of the animal throughout aging is different than the expression in the trunk. The terminal bulb of the *C. elegans* is located in the head, and therefore the expression of *elt-5* in the head of the worm is the relevant measurement that the terminal bulb muscle entropy should be compared against.

As reported by Budovskaya *et al.* (2008), the expression of *elt-5::cherry* reporter in the head of the *C. elegans* is upregulated between day two and day five, which corresponds to the leap found in this study between day two and day four. A sharper upregulation of *elt-5* is also noticeable between day seven and day 10. This finding is in agreement with the sharper leap of the measured texture entropy between days eight and 10. The expression remains steady in days five through seven, which corresponds to the negligible increase in the texture entropy during days four through eight.

The expression of *elt-3::GFP* reporter in the head of wild-type worms generally decreases as the *C. elegans* ages, but a deregulation of the gene is noticeable between day two and five, and between day nine and 12, while the expression in days seven through nine is nearly identical (Budovskaya *et al.*, 2008). These findings are also in agreement with the measurements of the texture entropy of the *C. elegans* terminal bulb. It should be noted, however, that *elt-3* expression deregulates also between day five and day seven. This deregulation of the expression of *elt-3::GFP* reporter does not have a corresponding increase in texture entropy of the terminal bulb during that period of the life of the *C. elegans*.

The agreement between the texture directionality and entropy and the age regulated gene expression indicates that the same distinct stages of the *C. elegans* aging that were deduced using DNA microarray experiments can also be identified by quantitative analysis of the tissue microscopy images of the worms.

While in many age regulated gene studies the age is measured by the chronological age (Lund *et al.*, 2002; Golden *et al.*, 2006; McColl *et al.*, 2008), the day of adulthood is not necessarily an

accurate indication of the physiological age of the animal. Since the texture entropy reflects age-related physiological changes, it is not unlikely that using the texture entropy instead of the chronological age can lead to a more accurate analysis of age regulated genes.

A widely held contention is that aging is a process driven by accumulated environmental damage, and there is evidence that damage accumulation such as oxidative damage (Lu *et al.*, 2004), protein glycation (Ulrich & Cerami, 2001), and inflammation (McGeer & McGeer, 2004) is related to aging in mammals. However, some organisms, such as *Homaridae* (lobsters), can live hundreds of years without showing any signs of decline that are typical to aging, observed in other closely related organisms that live in a similar environment (Guerin, 2007). In worms, there is no convincing evidence that the environmental damage can lead to conditions that have been associated with aging, such as the chronic induction of the stress responses (Lund *et al.*, 2002).

A different approach to aging is that the process is controlled by developmental pathways (Kirkwood & Rose, 1991; Williams, 1957). By measuring the alteration in the image texture entropy that noticeably changes throughout aging, we can identify several distinct states, separated by periods of rapid progression of aging. These findings are in agreement with age-regulated gene expression experiments, and indicate that the aging of *C. elegans* can be driven by developmental pathways rather than damage accumulation.

It should be noted, however, that the contention that developmental pathways run an “aging program” in *C. elegans* is controversial, and conflicting conclusions have been reported. For instance, Golden *et al.* (2008) studied whole-genome expression profiles of wild-type *C. elegans* throughout their entire life-span, and showed that gene expression changed gradually with the chronological and physiological (behavior) age. That work concluded that while the physiological age could be predicted using the expression of a large set of genes, no single gene could be reliably used as an aging biomarker, and after the age of 15 days gene expression profiles became more similar to each other and could not distinguish between younger and older animals.

*C. elegans* are physiologically very different from mammals, and therefore similar distinct stages of aging are not necessarily expected in humans based on these findings. However, some human aging researchers have proposed the contention that the human health shifts along a path of distinct states (Ferrucci *et al.*, 2008). Age-regulated gene expression in the cortex and medulla of the human kidney show similar aging profiles, suggesting that the aging of the kidney is controlled by biological mechanisms and pathways (Rod *et al.*, 2004). Clinical indicators such as motor unit characteristics (size and firing rate) provide evidence of a more rapid process of decline during the sixth decade of life (Ling *et al.*, 2009). While it is yet unknown whether these changes precede, follow, or occur concurrent to age-related modifications in muscle structure, it leaves the possibility that aging in humans does not progress at a constant rate throughout life, and that there are certain periods in life in which aging is more rapid.

## ACKNOWLEDGEMENT

**Funding:** This research was supported entirely by the Intramural Research Program of the National Institutes of Health, National Institute on Aging.

## REFERENCES

- Budovskaya, Y.V., Wu, K., Southworth, L.K., Jiang, M., Tedesco, P., Johnson, T.E. and Kim, S.K. (2008) An elt-3/elt-5/elt-6 GATA transcription circuit guides aging in *C. elegans*, *Cell*, **134**: 291–303.
- Duda, R. and Hart, P. (1973) *Pattern Classification and Scene Analysis*, John Wiley and Sons, pp. 271–272.
- Ferrucci, L., Giallauria, F. and Schlessinger, D. (2008) Mapping the road to resilience: Novel math for the study of frailty, *Mechanisms of Ageing and Development*, **129**: 677–679.
- Gabor, D. (1946) Theory of Communication, *Journal of IEEE*, **93**: 429–457.
- Garigan, D. et al. (2002) Genetic analysis of tissue aging in *Caenorhabditis elegans*: A role for heat-shock factor and bacterial proliferation, *Genetics*, **161**: 1101–1112.
- Golden, T.R. and Melov, S. (2006) Gene expression changes associated with aging in *C. elegans*. In The *C. elegans* Research Community (ed.), *WormBook* ed. The *C. elegans* Research Community, <http://www.wormbook.org>.
- Golden, T.R., Hubbard, A. and Melov, S. (2006) Microarray analysis of variation in individual aging *C. elegans*: Approaches and challenges, *Experimental Gerontology*, **10**: 1040–1045.
- Golden, T.R., Hubbard, A., Dando, C., Herren, M.A. and Melov, S. (2008) Age-related behaviors have distinct transcriptional profiles in *Caenorhabditis elegans*, *Aging Cell*, **7**: 850–865.
- Guerin, J.C. (2007) Emerging Area of Aging Research: Long-Lived Animals with Negligible Senescence, *Annals of the New York Academy of Sciences*, **1019**: 518–520.
- Helfrich, Y.R. et al. (2007) Effect of smoking on aging of photoprotected skin: evidence gathered using a new photometric scale, *Arch Dermatol*, **143**: 397–402.
- Herndon, L.A. et al. (2002) Stochastic and genetic factors influence tissue-specific decline in ageing *C. elegans*, *Nature*, **419**: 808–814.
- Haralick, R.M., Shanmugam, K. and Dinstein, I. (1973) Textural features for image classification, *IEEE Transactions on Systems, Man, and Cybernetics*, **6**, 269–285.
- Johnston, J., Iser, W.B., Chow, D.K., Goldberg, I.G. and Wolkow, C.A. (2008) Quantitative image analysis reveals distinct structural transitions during aging in *Caenorhabditis elegans* tissues, *PLoS ONE*, **3**, e2821.
- Kirkwood, T.B. and Rose, M.R. (1991) Evolution of senescence: late survival sacrificed for reproduction *Philosophical transactions: Biological Sciences*, **332**: 15–24.
- Lin, H.C., Chiu, C.Y. and Yang, S.N. (2003) Finding textures by textual descriptions, visual examples, and relevance feedbacks, *Pattern Recognition Letters*, **24**: 2255–2267.
- Ling, S.M., Conwit, P.A., Ferrucci, L. and Metter, E.J. (2009) Age-associated changes in motor unit physiology: Observations from the Baltimore Longitudinal Study of Aging, *Archives of Physical Medicine and Rehabilitation*, **90**: 1237–1240.
- Lu, T., Pan, Y., Kao, S.Y., Li, C., Kohane, I., Chan, J. and Yankner, B.A. (2004) Gene regulation and DNA damage in the ageing human brain, *Nature*, **429**: 883–891.
- Lund, J., Tedesco, P., Duke, K., Wang, J., Kim, S.K. and Johnson, T.E. (2002) Transcriptional profile of aging in *C. elegans*, *Current Biology*, **12**: 1566–1573.
- McCull, G., Killilea, D.W., Hubbard, A.E., Vantipalli, M.C., Melov, S., Lithgow, G.J. (2008) Pharmacogenetic analysis of lithium-induced delayed aging in *Caenorhabditis elegans*, *Journal of Biological Chemistry*, **283**: 350–357.
- McGeer, P.L. and McGeer, E.G. (2004) Inflammation and the degenerative disease of aging, *Annals of the New York Academy of Science*, **1035**: 104–116.
- Murphy, R.F., Velliste, M., Yao, J. and Porreca, G. (2001) Searching online journals for fluorescence microscopy images depicting protein subcellular location patterns, *Proc. 2nd IEEE Intl. Symp. on Bioinformatics and Biomedical Eng.*, 119–128.
- Rodwell, G.E., Sonu, R., Zahn, J.M., Lund, J., Wilhelm, J., Wang, L., Xiao, W., Mindrinos, M., Crane, E., Segal, E., Myers, B.D., Brooks, J.D., Davis, R.W., Higgins, J., Owen, A.B., Kim, S.K. (2004) A transcriptional profile of aging in the human kidney, *PLoS Biology*, **2**: e427
- Shamir, L., Orlov, N., Eckley, D.M., Macura, T., Johnston, J. and Goldberg, I.G. (2008) IICBU-2008 - A proposed benchmark suite for biological image analysis, *Medical & Biological Engineering & Computing*, **46**: 943–947.
- Shamir, L., Orlov, N., Eckley, D.M., Macura, T. and Goldberg, I.G. (2008) Wndchrm an open source utility for biological image analysis, *BMC Source Code for Biology and Medicine*, **3**: 13.
- Tamura, H., Mori, S. and Yamavaki, T. (1978) Textural features corresponding to visual perception, *IEEE Transactions On Systems, Man and Cybernetics*, **8**: 460–472.
- Ulrich, P. and Cerami, A. (2001) Protein glycation, diabetes, and aging, *Recent Prog. Horm. Res.*, **56**:1–21.
- Williams, G.C. (1957) Pleiotropy, natural selection, and the evolution of senescence, *Evolution*, **11**:398–411.
- Wolkow, C.A. (2006) Identifying factors that promote functional aging in *Caenorhabditis elegans*, *Exp Gerontol*, **41**: 1001–1006.